AGU PUBLICATIONS

Geophysical Research Letters

RESEARCH LETTER
10.1002/2017GL074866

Key Points:
- A single mantle plume can be responsible for two noncontemporaneous rift-to-spreading systems in a laterally nonhomogeneous lithosphere
- The prerift distance between a plume and a lateral lithospheric boundary between two segments controls rift-to-spreading systems
- The location of a plume with respect to lithosphere inhomogeneities is a key variable when modeling plume-induced continental break-up

Supporting Information:
- Supporting Information S1

Correspondence to:
A. Beniest,
anouk.beniest@etu.upmc.fr

Citation:
Beniest, A., Koptev, A., Leroy, S., Sassi, W., & Guichet, X. (2017). Two-branch break-up systems by a single mantle plume: Insights from numerical modeling. *Geophysical Research Letters*, *44*, 9589–9597. https://doi.org/10.1002/2017GL074866

Received 11 JUL 2017
Accepted 6 SEP 2017
Accepted article online 13 SEP 2017
Published online 4 OCT 2017

Two-Branch Break-up Systems by a Single Mantle Plume: Insights from Numerical Modeling

A. Beniest[1,2], A. Koptev[1,3], S. Leroy[1], W. Sassi[2], and X. Guichet[2]

[1]Sorbonne Universités, UPMC University Paris 06, ISTeP, CNRS-UMR, Paris, France, [2]IFP Energies nouvelles, Geosciences Division, Rueil-Malmaison, France, [3]Department of Geosciences, University of Tübingen, Tübingen, Germany

Abstract Thermomechanical modeling of plume-induced continental break-up reveals that the initial location of a mantle anomaly relative to a lithosphere inhomogeneity has a major impact on the geometry and timing of a rift-to-spreading system. Models with a warmer Moho temperature are more likely to result in "plume-centered" mode, where the rift and subsequent spreading axis grow directly above the plume. Models with weak far-field forcing are inclined to develop a "structural-inherited" mode, with lithosphere deformation localized at the lateral lithospheric boundary. Models of a third group cultivate two break-up branches (both "plume-centered" and "structural inherited") that form consecutively with a few million years delay. With our experimental setup, this break-up mode is sensitive to relatively small lateral variations of the initial anomaly position. We argue that one single mantle anomaly can be responsible for nonsimultaneous initiation and development of two rift-to-spreading systems in a lithosphere with a lateral strength contrast.

1. Introduction

Continental rifting is a complex process that depends on many factors such as the rheological structure of the crust and lithospheric mantle (Brun, 2002; Burov, 2011), thermal distribution in the lithosphere (Brune et al., 2014; Lavier & Manatschal, 2006), the presence or absence of inherited structures (Chenin & Beaumont, 2013; Manatschal et al., 2015), far-field forces (e.g., Huismans et al., 2001), and mantle plume(s) (Burov & Gerya, 2014). To date, a variety of analogue and numerical models have examined plume-induced continental rifting and break-up. For example, these models are able to explain quite complex geometries of a plume itself (Davaille et al., 2005) and its diverse effects when interacting with a rheologically stratified lithosphere such as asymmetric short-wavelength topography (Burov & Cloetingh, 2010; Burov & Gerya, 2014), the reduction of lithospheric strength (Brune et al., 2013), the multiphase development of rifting with a quick transition from wide to narrow mode (Koptev et al., 2017), and the shifted position of the break-up center with respect to the initial point of plume impingement (Beniest et al., 2017).

Single rift-plume interactions are well investigated, but complex multibranch continental rift and oceanic spreading systems are less well understood even though they exist all around the world. The Labrador Sea between Greenland and mainland Canada (Chalmers et al., 1995; Saunders et al., 1997) and the Aegir Ridge between Greenland and Norway (Gaina et al., 2009) are two (nonactive) spreading branches that developed consecutively in the North Atlantic region (Figure 1a, for tectonic reconstruction see Skogseid et al., 2000). The Abimael Ridge offshore south Brazil (Figure 1b, for tectonic reconstruction see, e.g., Torsvik et al., 2009 and Moulin et al., 2010), corresponds to an abandoned part of the South Atlantic rift system (Mohriak et al., 2010). Another example is the Tasman Sea that is separated by the Dampier Ridge from the Lord Howe Rise and Middleton Basin, all part of the same rift system (Figure 1c, for tectonic reconstruction see Gaina et al., 1998). These ridges and branches differ significantly in terms of the width of newly formed oceanic lithosphere and the distance between active and aborted ridges. For example, the total width of the Norwegian-Greenland Sea reaches for some 1000 km (Figure 1a, Greenhalgh & Kusznir, 2007) whereas both the Labrador and Tasman Sea only gained hundreds of kilometers of oceanic crust width before abortion (Figures 1a and 1c). The oceanic lithosphere associated with the Abimael ridge is even narrower than the Labrador Sea and the Tasman Sea, with a total width of a couple of tens of kilometers only (Figure 1b, Mohriak et al., 2010). The Lord Howe Rise and Middleton Basin (Figure 1c) have only reached a rift phase (between 90 Ma and 84 Ma, Gaina et al., 1998), not providing any evidence for oceanic crust formation, but they remain a separate branch of the break-up system of the Tasman Sea, where oceanic spreading initiated at 83 Myr (Gaina et al., 1998). The distance between the present-day location of the aborted and active rift and spreading ridges can be as far away as over 5000 km in the case of the Abimael ridge and

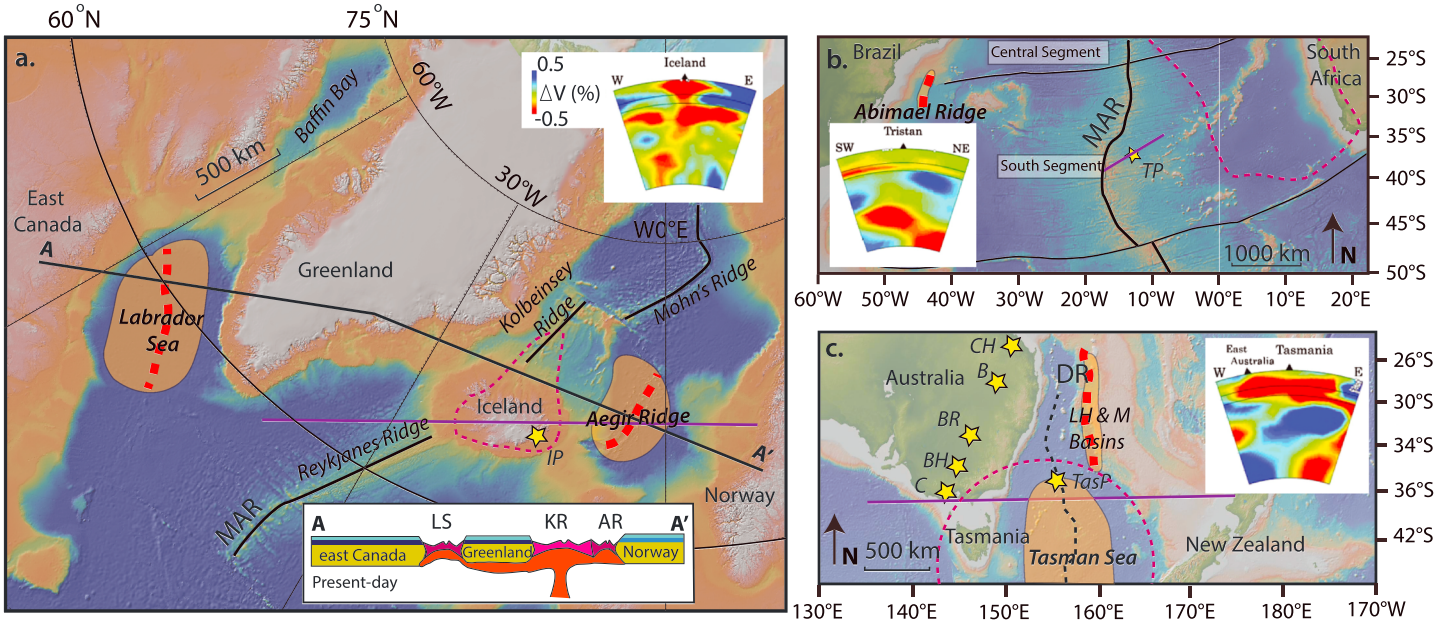

Figure 1. Three natural examples of a complex multibranch spreading system associated with a single mantle plume: (a) the Labrador Sea (Chalmers et al., 1995) and the Aegir Ridge (Greenhalgh & Kusznir, 2007) developed consecutively in the North Atlantic region. The Iceland plume (dashed purple line) is now located directly below currently active mid-ocean ridge (Rickers et al., 2013). The black line represents a position of a schematic cross section of the North Atlantic domain (for color code see Figures 2 and 4). (b) the Abimael Ridge is a failed rift branch along which evidence for oceanic crust has been observed (e.g., Mohriak et al., 2010). The Tristan Plume associated to the African Superswell (dashed purple line) is located close to the South Atlantic mid-ocean ridge (Ernesto et al., 2002). (c) The spreading axes of the Tasman Sea and rift axis of Lord Howe and Middleton Basins are part of the same system (Gaina et al., 1998). The Tasmantid (TasP) and Cosgrove (C) hotspots lay on the edge of the Tasmantid Plume (dashed purple line). The tomographic images are taken from Zhao (2007). The purple lines show their approximate location. The yellow stars are asthenosphere hotspot locations. IP = Iceland Plume hotspot, LS = Labrador Sea, KR = Kolbeinsey Ridge, AR = Aegir Ridge, MAR = Mid-Atlantic Ridge, TP = Tristan Plume hot spot, BH = Begargo Hill hotspot, BR = Bokhara River hot spot, B = Buckland Hot spot, CH = Cape Hillsborough hot spot, DR = Dampier Ridge, LH&M Basins = Lord Howe and Middleton Basins. Australian hot spots after Davies et al. (2015).

the South Atlantic mid-ocean ridge (Figure 1b) or as close by as only 200 km in case of the Aegir ridge (Figure 1a). Despite these differences, such multibranch systems have one important thing in common: they are underlain by a deep-rooted mantle anomaly with varying geometries that may have triggered their initiations and controlled their subsequent evolution. Present-day geometries of mantle anomalies can be visualized with mantle tomography. This method suggests that the Iceland plume (Figure 1a, after Zhao, 2007) extends throughout the mantle to the core-mantle boundary (French & Romanowicz, 2015). The Tristan plume (Figure 1b, Zhao, 2007) is rooted in the lower mantle and seems to be failing in the upper mantle nowadays, although it leaves an ancient hot spot trail behind (Schlömer et al., 2017). The Tasmantid (TasP) low velocity zone (Figure 1c, Zhao, 2007) is currently confined to the upper mantle and transition zone with a lower mantle stem significantly distanced from the upper mantle part of the plume. Yet up to five ancient hot spots could be the surface expressions of this mantle plume (Davies et al., 2015).

Despite numerous numerical modeling exercises (Beniest et al., 2017; Brune et al., 2014; Burov & Gerya, 2014; Chenin & Beaumont, 2013; Huismans & Beaumont, 2008; Koptev et al., 2016; Lavecchia et al., 2017), no self-consistent numerical model has thus far explained how multibranch break-up centers, separated in space and time, can result from the impact of the same mantle plume (Figure 1). Here we present the results of a 2-D thermomechanical modeling study investigating the effect of the prerift position of a mantle plume anomaly on the rift-to-spreading evolution in a laterally heterogeneous lithosphere, with different initial Moho temperatures and various extension rates.

2. Numerical Model Setup

We use a 2-D version of the viscous-plastic numerical code I3ELVIS (Gerya & Yuen, 2007) to study plume-induced rifting and continental break-up of a lithosphere with a lateral rheological contrast. This code

combines a finite difference method on a staggered Eulerian grid with a marker-in-cell technique. For a detailed description of the code we refer to Gerya and Yuen (2007), Gerya (2010), and supporting information text S1.

The spatial dimensions of the model are 1500 km in length and 635 km in width. The model box contains 297 × 133 nodes, so that the grid cell size corresponds to 5 × 5 km. The model setup consists of a three-layered lithosphere (150 km), overlying the sublithospheric mantle (455 km). The crustal thickness is 40 km, equally divided in upper crust (20 km) and lower crust (20 km) (supporting information S1, Figure 1.1). The homogenous upper crust has ductile properties of wet quartzite whereas the lower crust is characterized by a lateral contrast in rheological strength: a "strong" left side, made of anorthite rheology, and a "weak" right side, consisting of wet quartzite rheology (Bittner & Schmeling, 1995; Clauser & Huenges, 1995; Connolly, 2005; Kohlstedt et al., 1995; Ranalli, 1995; Turcotte & Schubert, 2002). The contact between these two rheologically different crustal segments represents a simplified inherited structure, located in the top-middle of the model box. The lithospheric and sublithospheric mantle uses dry olivine rheology whereas the mantle plume is simulated with wet olivine rheology (more detailed information on rheological and material properties of the crust and mantle can be found in supporting information S2 table 2.1). The initial mantle plume anomaly is positioned at the base of the model box and has a spherical shape with a radius of 200 km, which is in correspondence with previous work (e.g., Burov & Gerya, 2014; Koptev et al., 2015). We use a linear geotherm with 0°C at the surface, 500°C or 600°C at the Moho (40 km), 1300°C at the base of the lithosphere (150 km), and 1630°C at the bottom of the model domain (635 km). The Moho temperature (500°C and 600°C) is one of the variable parameters of our study (supporting information S3 table 3.1). The mantle anomaly has an initial temperature of 2000°C corresponding to 300–370°C contrast with surrounding mantle. The general thermal boundary conditions align with fixed temperatures at the top (0°C) and bottom (1630°C) of the model and zero heat flux is imposed on the vertical boundaries of the model box. Far-field tectonic extension is applied on both vertical sides with a constant half-rate of 5 mm/yr or 10 mm/yr (supporting information S3 table 3.1). The resulting horizontal forces along the border of the models are of the same order of magnitude (5×10^{12} N per unit length) as "ridge push" (e.g., Buck, 2007) and "slab-pull" forces (Schellart, 2004). Apart from the initial Moho temperature and the initial extension rate, our main changing parameter is the prerift plume location. In a previous study of Beniest et al. (2017) the anomaly was positioned at three different locations with respect to the crustal rheological and geometrical variations. For this study, the mantle plume is initially placed directly below the rheological contact after which it is positioned further away from this contact below the stronger half of the model with steps of 25–100 km. The maximum lateral shift of the plume with respect to its central location is 450 km. We performed three sets of nine numerical experiments, resulting in 27 models total (supporting information S3 table 3.1). The first set has a Moho temperature of 500°C and an extension half-rate of 10 mm/yr, the second set has a Moho temperature of 600°C and an extension half-rate of 10 mm/yr, and the last set has a Moho temperature of 500°C and an extension half-rate of 5 mm/yr. In addition, we performed 19 complementary models (supporting information S3 table 3.2 and S4 figures 4.1–4.5) to test the models sensitivity to certain parameters such as grid cell size (higher resolution), plume size (larger radius), plume temperature (1900°C instead of 2000°C), Moho isotherm (650°C), and more complex structure of the lithospheric mantle (different thicknesses for stronger and weaker segments) and crustal geotherm (nonlinear).

3. Experimental Results

In all models the mantle plume rises rapidly, reaching the base of the lithosphere in less than 2 Myr. Plume material spreads laterally along the lowest part of the lithosphere flowing as far away as ~1000 km (similarly to previous 2-D experiments of Burov & Cloetingh, 2010 and 3-D models of Koptev et al., 2017). Unlike these models, our experiments develop different rift-to-break-up modes that can be divided into three major groups (Figure 2 and supporting information S3 table 3.1).

The first group demonstrates continental break-up directly above the initial plume location ("plume-centered" break-up mode, model 8, Figure 2d and supporting information S5 figure 5.1d). This category corresponds to the classical plume models also shown by, for example, Burov and Cloetingh (2010) and d'Acremont et al. (2003). Despite initial deformation localization at the contact between the weak and strong segments ("structural-inherited") (supporting information S5 figure 5.1d; 1 Myr), vertical ascent of hot plume

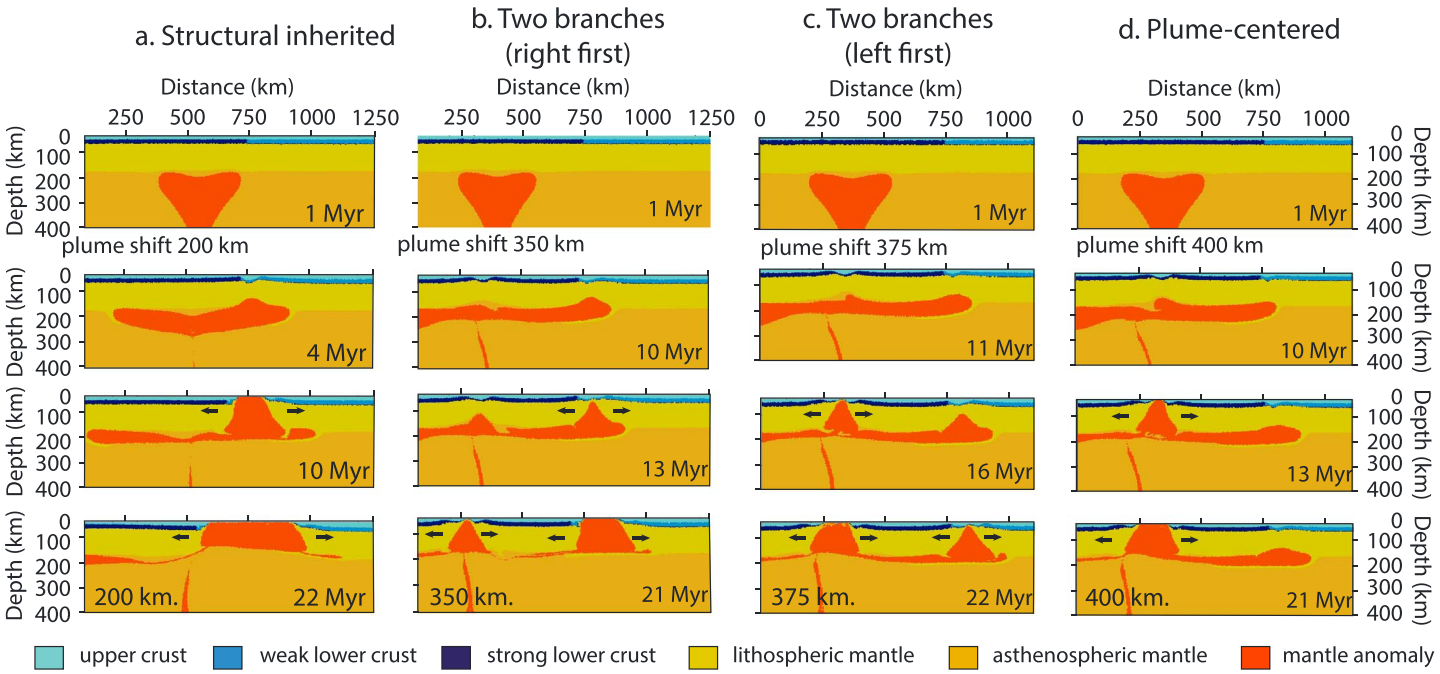

Figure 2. The most representative examples of the three different break-up modes (from the model series distinguished with a Moho temperature of 500°C and half-rate extension of 10 mm/yr, see also Figure 3a and supporting information S2 table 2.1): (a) model 3 with an initial plume shift towards the stronger segment of 200 km: "structural inherited" mode; (b and c) model 6 (plume shift of 350 km) and model 7 (plume shift of 375 km): "two-branch"; (d) model 8 (plume shift of 400 km): "plume-centered" mode. Note that not only the initial position but also the initial size (models 37 and 38) and temperature (models 39–42) of the mantle anomaly (supporting information S4 figures 4.3 and 4.4) might be critical for the final break-up mode.

material throughout the lithospheric mantle (Figure 2d; 10 Myr) leads to a second "plume-centered" zone of localized strain (supporting information S5 figure 5.1d; 10 Myr). This zone becomes the dominant deformation domain (supporting information S5 figure 5.1d; 13 Myr) at the moment of the continental break-up (Figure 2d; 13 Myr). The initial structurally inherited deformation zone becomes eventually completely extinct (supporting information S5 figure 5.1d; 21 Myr). Thus, the plume material flowing laterally at the base of the lithosphere is unable to turn the distant structurally inherited rifting into a break-up center (supporting information S5 figure 5.1d).

The second category includes models showing rifting and subsequent break-up only at the contact between two rheological segments ("structural inherited" break-up mode). Here, due to the initial plume position being closer to the inherited structure, localized plume ascent coincides with the structurally inherited zone of the initial continental rift. This leads to plume-induced (but structurally inherited) break-up (model 3, Figure 2a). Note that there is no evidence for strain localization within the stronger lithosphere above the initial plume location (supporting information S5 figure 5.1a).

Models of the third group illustrate an intermediate behavior where two break-up centers form consecutively. These "two-branch" experiments develop first the "structural inherited" and then the "plume-centered" break-up modes or vice versa depending on the initial plume position (models 6 and 7, Figures 2b and 2c). In both cases the first rifting phase is structurally inherited (supporting information S5 figures 5.1b and 5.1c; 1 Myr), but the order in which the break-up centers develop depends heavily on relatively small ($<$30 km) lateral variation of the initial plume position with respect to the rheological boundary (Figures 2b and 2c and supporting information S5 figures 5.1b and 5.1c). When the initial thermal anomaly is situated farther away from the rheological contact (at 375 km), "plume-centered" break-up develops first, directly above the anomaly. This is due to the rapid, localized ascent of plume material through the mantle part of the stronger overlying lithosphere (Figure 2c and supporting information S5 figure 5.1c, 11–16 Myr). After that, hot plume material residing at the base of the lithosphere rises below the structurally inherited rift zone (Figure 2c and supporting information S5 figure 5.1c; 16 Myr) leading to complete rupture of the continent at the preimposed structural boundary (Figure 2c and supporting information S5 figure 5.1c; 22 Myr).

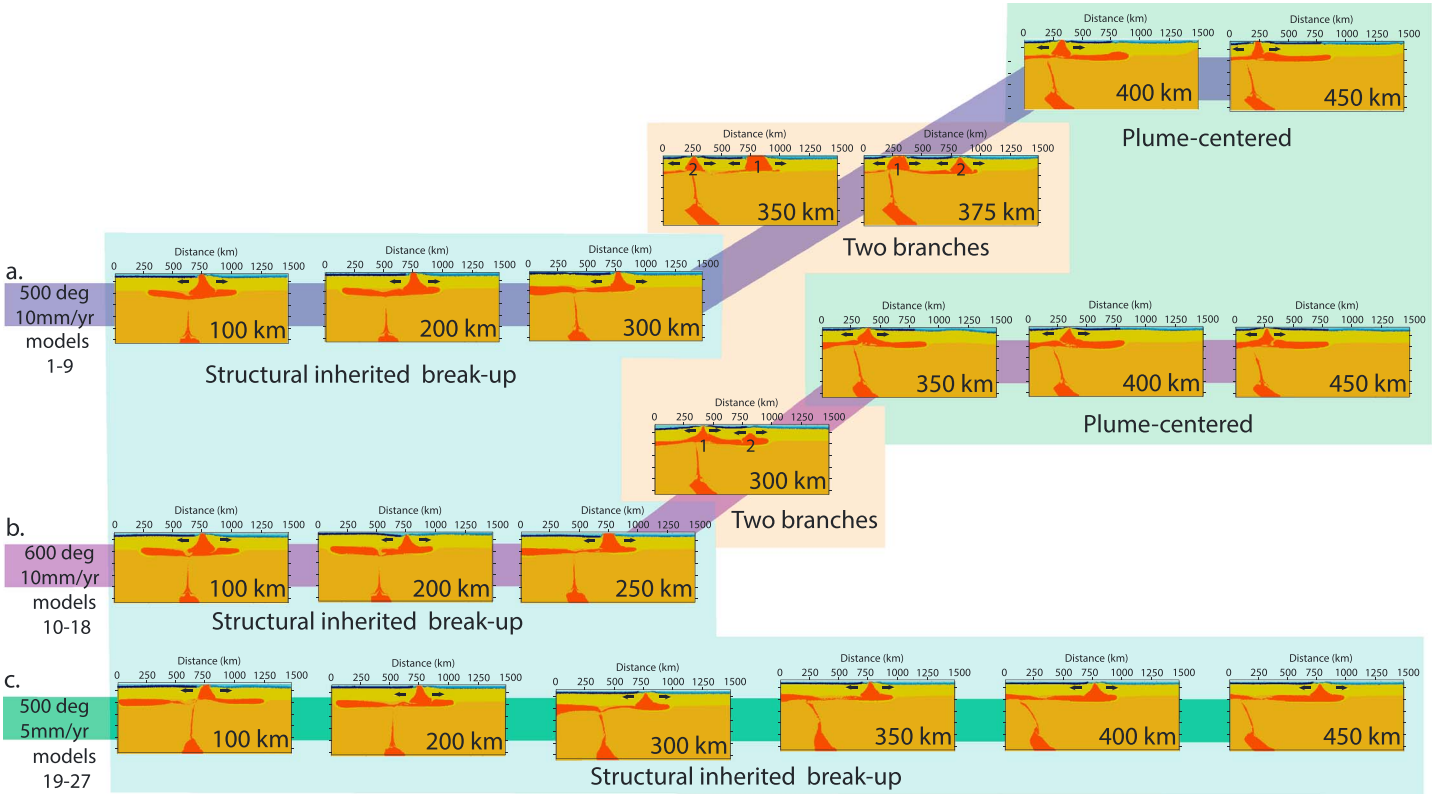

Figure 3. Graph showing the results of the three sets of models (a) 500°C Moho temperature and 10 mm/yr extension half-rate, (b) 600°C Moho temperature and 10 mm/yr extension half-rate, and (c) 500°C Moho temperature and 5 mm/yr extension rate) aligned with increasing distance between the initial anomaly location and the rheological contact. For the experiments with faster extension half-rate (10 mm/yr) there is a critical distance when the system changes from "structural inherited" to "plume-centered" break-up through a two-branch system. This distance is (a) between 300 and 400 km for the Moho temperature of 500°C and (b) between 250 and 350 km for Moho temperature of 600°C. Closer to the rheological boundary, the rift-to-spreading system develops uniquely above the structural inheritance; farther away, it evolves directly above the plume impingement point. Note that a "plume-centered" mode of development does not exclude some localization of initial deformation at the rheological contact (structurally inherited aborted rifting, see supporting information S5 Figure 5.1).

When the mantle plume is positioned only 350 km away from the rheological contact, "structural inherited" break-up develops first, followed by a "plume-centered" one (Figure 2b and supporting information S5 figure 5.1b). In both cases the time delay between these two continental break-ups is less than 10 Myr.

The "two-branch" category results from the reference model setup that uses a relatively fast extension rate (half-rate 10 mm/yr) and colder Moho temperature (500°C, models 1–9, Figure 3a). In a different set of models where the extension half-rate is being kept at 10 mm/yr but the crustal geotherm is warmer (600°C at the Moho, models 10–18), a similar two branch system is produced when the plume is shifted 300 km away from the rheological contact (Figure 3b). Note, however, that in this model, only the "plume-centered" rift axis evolves into a spreading center, whereas the "structural inherited" branch does not reach this phase. For this set of model setups, the "plume-centered" break-up mode is the dominant break-up mechanism when the anomaly is located 350 km or farther away from the inherited structure (Figure 3b). A series of complementary experiments show that a further increase in the initial crustal geotherm (e.g., 650°C, models 30–36) has no principal effect on the final continental break-up mode (compare Figure 3b and supporting information S4 figure 4.2). Small variations in the initial temperature distribution, for example, a nonlinear crustal geotherm that takes into account radiogenic heat production (model 29, supporting information S4 figure 4.1), do not play a significant role neither. For the last set of models the thermal state is the same as for the reference model (500°C Moho temperature) and the spreading rate is decreased to 5 mm/yr half-rate extension (models 19–27). For this model series, all models persistently cultivate "structural inherited" break-up for all tested mantle plume emplacements (Figure 3c). Exactly the same behavior is observed in the complementary experiments that include nonuniform thicknesses of the lithosphere with a thicker stronger (150 km)

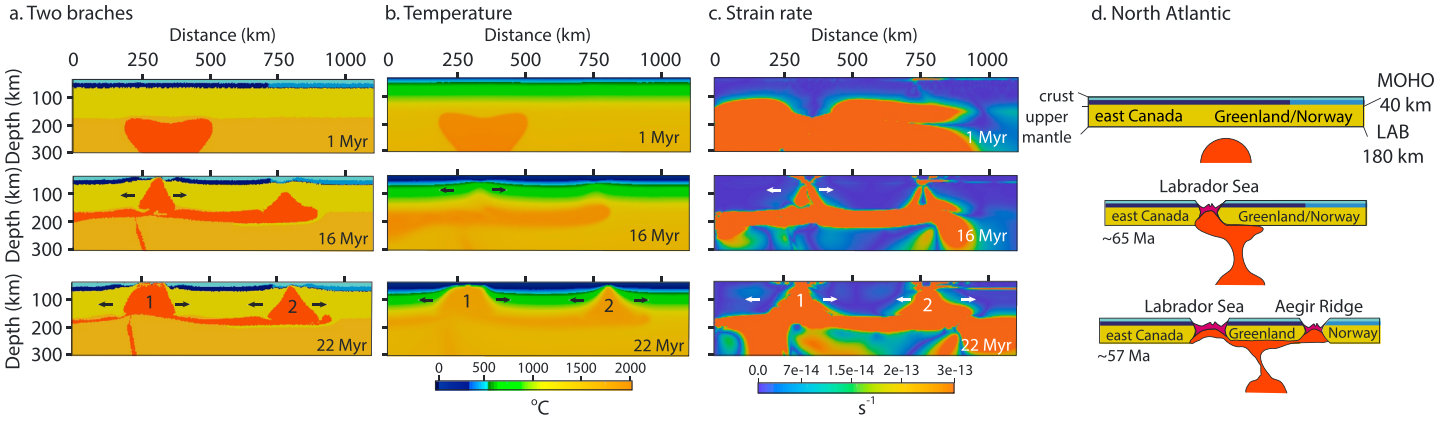

Figure 4. (a) Phase, (b) temperature and (c) strain rate plots of model 7 (Moho temperature of 500°C, extension half-rate of 10 mm/yr, plume shift of 375 km). This model develops a "two-branch" break-up mode and bears strong similarities with the geodynamical evolution in the North Atlantic domain (d, schematic representation): (1) the first branch forms in the left part of the model, corresponding to the strong crust, similar to Greenland craton that will eventually separate Greenland and Canada (Peace et al., 2016); and (2) the second branch forms 6 Myr later close to the inherited structure, comparable to the break-up of the Caledonian orogeny eventually separating Greenland and Norway (Lundin & Doré, 2002). The pink color on the schematic profiles refers to newly formed oceanic lithosphere.

segment and a thinner weaker (100 km) segment (models 43–46). Regardless the initial plume position and the type of transitional zone between the different rheological segments (vertical or slope), these models show only "structural inherited" break-up mode, without any evidence for "plume-centered" rift initiation (supporting information S4 figure 4.5). Without dismissing that such contrasts in the rheological and thermal structure are present not only at crustal level but also in the lithospheric mantle, our results provide new elements to evaluate the importance of the mantle inhomogeneities on the initiation and development of multibranch rift systems.

4. Discussion and Conclusion

Our results show that in case of a cold Moho (500°C) and relatively fast (10 mm/yr) extension, three modes of break-up are possible, depending on the location of the mantle anomaly with respect to a rheological contact. With respect to this "reference model" set, a higher Moho temperature better facilitates deeper penetration of plume material into the lithosphere. This favors a vertical localized ascent up to the Moho ultimately leading to continental break-up directly above initial plume emplacement. This "plume-centered" axis is situated closer to the rheological contact than in case of a lower Moho temperature. A general example of this "plume-centered" rifting can be observed in, for example, the Afar depression where the formation of complex triple junction (e.g., McClusky et al., 2010) is linked to the arrival of the Afar plume (Bellahsen et al., 2003) at ~30 Ma (Coulié et al., 2003; Hofmann et al., 1997). In case of a relatively low extension half-rate (5 mm/yr), the thermal impact of the mantle plume becomes less important; the system prefers deformation localization at the mechanical instability created by the rheological contact. This implies that external tectonic forcing is too weak to localize deformation outside of the predefined structural boundary even in presence of an active mantle anomaly that is considerably shifted with respect to this structure. This is generally consistent with numerical results done by Burov and Gerya (2014).

A natural example for "structural inherited" break-up could be the South Atlantic domain where "plume-induced" break-up takes place at the boundary between stronger (African) and weaker (South American) lithosphere segments despite the possible eastward offset initial position of the mantle plume with respect to this boundary (see Beniest et al., 2017 for more details).

When the anomaly is located at a position where both the impact of the mantle anomaly on the lithosphere and the predefined rheological contact of the system are competing for deformation localization, the "two-branch" break-up mode develops. For our set of reference models (Figure 3a), a two-branch system forms when the mantle anomaly has a lateral displacement of 350–375 km towards the stronger half of the model domain with respect to the rheological contact. The two branches develop consecutively, with roughly 10 Myr delay, with either "structural inherited" break-up first, followed by "plume-centered" (displacement

350 km, Figure 2b) or the other way around (displacement 375 km, Figure 2c). Slight offset to this specific dislocation converts the break-up mode to either "structural inherited" or "plume-centered" (Figures 2 and 3).

Both "plume-centered" and "structural inherited" modes of break-up have been modeled by Beniest et al. (2017) and Lavecchia et al. (2017). To model a two-branch system, a particular position of the mantle plume anomaly with respect to a rheological contrast at crustal level should be determined. Only a relatively narrow (25–50 km) range of initial plume locations can result in multibranch systems associated with the direct impact of locally upwelled plume material. The thermal state appears to be of lesser importance (see Figures 3a and 3b where two branches develop with both colder and hotter Moho temperatures), but far-field forcing should not be too weak (see Figure 3c). Our "two-branch" model with a plume location 375 km away from the rheological contact bears most similarities to the geodynamic history of the North Atlantic region (Figure 4). Here the old and rigid lithosphere of the Greenland craton (Kerr et al., 1997) was underlain by a single mantle anomaly (the Iceland mantle plume) before rifting started in the Labrador Sea (Lundin & Doré, 2002; Rogozhina et al., 2016). The old craton was subjected to plume-activated continental rifting in the Late Triassic or Jurassic followed by seafloor spreading with the oldest accepted magnetic anomaly being of Danian (~64 Ma) age (Chalmers et al., 1995) (although older anomalies are still a matter of debate, Peace et al., 2016). Note, however, that the opening of the mostly a magmatic Labrador Sea might have started before the mantle plume impacted the lithosphere beneath West Greenland (Larsen & Saunders, 1998). A second axis of active spreading (the Aegir Ridge) initiated around 57 Ma (i.e., 5–10 Myr later)(Lundin & Doré, 2002; Peace et al., 2016) close to the adjacent Caledonian suture zone (Abdelmalak et al., 2016; Gaina et al., 2009), several hundreds of kilometers away from the area of the first plume impingement. Thus, both the position of the Iceland plume (e.g., Rogozhina et al., 2016, and references herein) near the western coast of Greenland (with a shift of several hundreds of kilometers with respect to the weaker Caledonian suture) at the moment of the initiation of the first spreading branch (even if the paleoposition of the Iceland hot spot remains debatable—see, e.g., Torsvik et al., 2015) and the time delay of less than 10 Myr between plume-induced and structurally inherited break-ups bear strong similarity with the key features of our two-branch model displayed in Figures 2c and 4a–4c. In this case, the key features refer to (1) a lateral varying rheological contact resembling an inherited structure (the Caledonian suture), (2) a relatively cool thermal structure comparable to a craton (West-Canada-Greenland craton), (3) the location of the mantle anomaly at 350–375 km away from the inherited structure, which would be well below the Greenland craton, and (4) the timing of the two break-up branches only 5–10 Myr apart in the model, which corresponds well to the 64 Ma for the Labrador Sea ("plume-centered" break-up branch) and 7 Myr later, at 57 Ma the Aegir Ridge ("structural inherited" break-up branch). We note that given the natural limitations of the used 2-D approach, further exploring the effect plumes have on multibranch systems with 3-D tests would facilitate a more detailed comparison with observations in the North Atlantic.

Based on our modeling results and examples from nature, we note that rheological heterogeneities in the lithosphere, its thermal state and acting mechanical forces are important parameters for the rift-to-break-up evolution of the system. In addition, we show that the initial location of the plume with respect to a laterally varying lithosphere is not only an important factor for rift and break-up styles and geometries but also affects the timing and order of the development of the branches. We argue that in combination with far-field forces and the thermal state of the system, the emplacement of the plume anomaly is a key parameter for numerical modelling of plume-induced continental rifting and break-up.

Acknowledgments
This study is cofunded by the Advanced ERC grant 290864 RHEOLITH to Alexander Koptev. Anouk Beniest is funded by IFP Energies nouvelles. The numerical simulations were performed on the ERC-Rheolith funded SGI Ulysse cluster of ISTeP. We thank Taras Gerya for providing the numerical code I3ELVIS. The figures in the supporting information contain the numerical simulation data.

References

Abdelmalak, M. M., Planke, S., Faleide, J. I., Jerram, D. A., Zastrozhnov, D., Eide, S., & Myklebust, R. (2016). The development of volcanic sequences at rifted margins: New insights from the structure and morphology of the Vøring Escarpment, mid-Norwegian Margin. *Journal of Geophysical Research: Solid Earth*, *121*, 5212–5236. https://doi.org/10.1002/2015JB012788

Bellahsen, N., Faccenna, C., Funiciello, F., Daniel, J. M., & Jolivet, L. (2003). Why did Arabia separate from Africa? Insights from 3-D laboratory experiments. *Earth and Planetary Science Letters*, *216*, 365–381. https://doi.org/10.1016/S0012-821X(03)00516-8

Beniest, A., Koptev, A., & Burov, E. (2017). Numerical models for continental breakup: Implications for the South Atlantic. *Earth and Planetary Science Letters*, *461*, 176–189. https://doi.org/10.1016/j.epsl.2016.12.034

Bittner, D., & Schmeling, H. (1995). Numerical modelling of melting processes and induced diapirism in the lower crust. *Geophysical Journal International*, *123*, 59–70.

Brun, J.-P. (2002). Deformation of the continental lithosphere: Insights from brittle-ductile models. *Geological Society of London, Special Publication*, *200*(1), 355–370. https://doi.org/10.1144/GSL.SP.2001.200.01.20

Brune, S., Popov, A. A., & Sobolev, S. V. (2013). Quantifying the thermo-mechanical impact of plume arrival on continental break-up. *Tectonophysics*, *604*, 51–59. https://doi.org/10.1016/j.tecto.2013.02.009

Brune, S., Heine, C., Pérez-Gussinyé, M., & Sobolev, S. V. (2014). Rift migration explains continental margin asymmetry and crustal hyper-extension. *Nature Communications*, *5*(4014), 1–9. https://doi.org/10.1038/ncomms5014

Buck, W. R. (2007). Dynamic processes in extensional and compressional settings: The dynamics of continental breakup and extension. *Treatise on Geophysics*, *6*, 335–376. https://doi.org/10.1016/B978-044452748-6.00110-3

Burov, E., & Cloetingh, S. (2010). Plume-like upper mantle instabilities drive subduction initiation. *Geophysical Research Letters*, *37*, L03309. https://doi.org/10.1029/2009GL041535

Burov, E., & Gerya, T. (2014). Asymmetric three-dimensional topography over mantle plumes. *Nature*, *513*, 85–89. https://doi.org/10.1038/nature13703

Burov, E. B. (2011). Rheology and strength of the lithosphere. *Marine and Petroleum Geology*, *28*, 1402–1443. https://doi.org/10.1016/j.marpetgeo.2011.05.008

Chalmers, J. A., Larsen, L. M., & Pedersen, A. K. (1995). Widespread Palaeocene volcanism around the northern North Atlantic and Labrador Sea: Evidence for a large, hot, early plume head. *Journal of the Geological Society of London*, *152*(1992), 965–969.

Chenin, P., & Beaumont, C. (2013). Influence of offset weak zones on the development of rift basins: Activation and abandonment during continental extension and breakup. *Journal of Geophysical Research: Solid Earth*, *118*, 1698–1720. https://doi.org/10.1002/jgrb.50138

Clauser, C., & Huenges, E. (1995). Thermal conductivity of rocks and minerals, *Rock Physics & Phase Relations: A Handbook of Physical Constants, ref*. Shelf *3*, 105–126.

Connolly, J. A. D. (2005). Computation of phase equilibria by linear programming: A tool for geodynamic modeling and its application to subduction zone decarbonation. *Earth and Planetary Science Letters*, *236*, 524–541. https://doi.org/10.1016/j.epsl.2005.04.033

Coulié, E., Quidelleur, X., Gillot, P., Courtillot, V., Lefèvre, J.-C., & Chies, S. (2003). Comparative K - Ar and Ar / Ar dating of Ethiopian and Yemenite Oligocene volcanism: Implications for timing and duration of the Ethiopian traps. *Earth and Planetary Science Letters*, *206*, 477–492.

D'Acremont, E., Leroy, S., & Burov, E. B. (2003). Numerical modelling of a mantle plume: The plume head–lithosphere interaction in the formation of an oceanic large igneous province. *Earth and Planetary Science Letters*, *206*, 379–396. https://doi.org/10.1016/S0012-821X(02)01058-0

Davaille, A., Stutzmann, E., Silveira, G., Besse, J., & Courtillot, V. (2005). Convective patterns under the Indo-Atlantic «box». *Earth and Planetary Science Letters*, *239*(3–4), 233–252. https://doi.org/10.1016/j.epsl.2005.07.024

Davies, D. R., Rawlinson, N., Iaffaldano, G., & Campbell, I. H. (2015). Lithospheric controls on magma composition along Earth's longest continental hotspot track. *Nature*, *525*(7570), 511–514. https://doi.org/10.1038/nature14903

Ernesto, M., Marques, L. S., Piccirillo, E. M., Molina, E. C., Ussami, N., Comin-Chiaramonti, P., & Bellinie, G. (2002). Paraná Magmatic Province- Tristan da Cunha plume system: fixed versus mobile plume, petrogenetic considerations and alternative heat sources. *Journal of Volcanology and Geothermal Research*, *118*, 15–36.

French, S. W., & Romanowicz, B. (2015). Broad plumes rooted at the base of the Earth's mantle beneath major hotspots. *Nature*, *525*(7567), 95–99. https://doi.org/10.1038/nature14876

Gaina, C., Roest, W. R., Müller, R. D., & Symonds, P. (1998). The opening of the Tasman Sea: a gravity anomaly animation. *Earth Interactions*, *2*(4), 1–23.

Gaina, C., Gernigon, L., & Ball, P. (2009). Palaeocene—Recent plate boundaries in the NE Atlantic and the formation of the Jan Mayen microcontinent. *Journal of the Geological Society of London*, *166*, 601–616. https://doi.org/10.1144/0016-76492008-112

Gerya, T. (2010). Dynamical instability produces transform faults at mid-ocean ridges. *Science*, *329*(5995), 1047–1050.

Gerya, T. V., & Yuen, D. A. (2007). Robust characteristics method for modelling multiphase visco-elasto-plastic thermo-mechanical problems. *Physics of the Earth and Planetary Interiors*, *163*, 83–105. https://doi.org/10.1016/j.pepi.2007.04.015

Greenhalgh, E. E., & Kusznir, N. J. (2007). Evidence for thin oceanic crust on the extinct Aegir Ridge, Norwegian Basin, NE Atlantic derived from satellite gravity inversion. *Geophysical Research Letters*, *34*, L06305. https://doi.org/10.1029/2007GL029440

Hofmann, C., Courtillot, V., Féraud, G., Rochette, P., Yirgu, G., Ketefo, E., & Pik, R. (1997). Timing of the Ethiopian flood basalt event and implications for plume birth and global change. *Nature*, *389*, 838–841. https://doi.org/10.1038/39853

Huismans, R. S., & Beaumont, C. (2008). Complex rifted continental margins explained by dynamical models of depth-dependent lithospheric extension. *Geology*, *36*(2), 163–166. https://doi.org/10.1130/G24231A.1

Huismans, R. S., Podladchikov, Y. Y., & Cloetingh, S. (2001). Transition from passive to active rifting: Relative importance of asthenospheric doming and passive extension of the lithosphere. *Journal of Geophysical Research*, *106*, 11,271–11,291.

Kerr, A., Hall, J., Wardle, R. J., Gower, C. F., & Ryan, B. (1997). Early Proterozoic belts Ketilidian. *Tetonics*, *16*, 942–965.

Kohlstedt, D. L., Evans, B., & Mackwell, S. J. (1995). Strength of the lithosphere: Constraints imposed by laboratoy experiments. *Journal of Geophysical Research*, *100*, 17,587–17,602.

Koptev, A., Calais, E., Burov, E., Leroy, S., & Gerya, T. (2015). Dual continental rift systems generated by plume – lithosphere interaction. *Nature Geoscience*, *8*, 388–392. https://doi.org/10.1038/NGEO2401

Koptev, A., Burov, E., Calais, E., Leroy, S., Gerya, T., Guillou-Frottier, L., & Cloetingh, S. (2016). Contrasted continental rifting via plume-craton interaction: Applications to Central East African Rift. *Geoscience Frontiers*, *7*, 221–236. https://doi.org/10.1016/j.gsf.2015.11.002

Koptev, A., Burov, E., Gerya, T., Le, L., Leroy, S., Calais, E., & Jolivet, L. (2017). Plume-induced continental rifting and breakup in ultra-slow extension context: Insights from 3D numerical modeling. *Tectonophysics*, 1–17. https://doi.org/10.1016/j.tecto.2017.03.025

Larsen, H. C., & Saunders, A. D. (1998). Tectonism and volcanism at the southeast Greenland rifted margin: A record of plume impact and later continental rupture. *Proceedings of the Ocean Drilling Program, Scientific Results*, *152*, 503–533. https://doi.org/10.2973/odp.proc.sr.152.1998

Lavecchia, A., Thieulot, C., Beekman, F., Cloetingh, S., & Clark, S. (2017). Lithosphere erosion and continental breakup: Interaction of extension, plume upwelling and melting. *Earth and Planetary Science Letters*, *467*, 89–98. https://doi.org/10.1016/j.epsl.2017.03.028

Lavier, L. L., & Manatschal, G. (2006). A mechanism to thin the continental lithosphere at magma-poor margins. *Nature*, *440*(7082), 324–328. https://doi.org/10.1038/nature04608

Lundin, E., & Doré, A. G. (2002). Mid-Cenozoic post-breakup deformation in the "passive" margins bordering the Norwegian - Greenland Sea. *Marine and Petroleum Geology*, *19*, 79–93.

Manatschal, G., Lavier, L., & Chenin, P. (2015). The role of inheritance in structuring hyperextended rift systems: Some considerations based on observations and numerical modeling. *Gondwana Research*, *27*(1), 140–164. https://doi.org/10.1016/j.gr.2014.08.006

McClusky, S., Reilinger, R., Ogubazghi, G., Amleson, A., Healeb, B., & Vernant, P. (2010). Kinematics of the southern Red Sea–Afar Triple Junction and implications for plate dynamics, *Geophysical Research Letters*, *37*, L05301. https://doi.org/10.1029/2009GL041127

Mohriak, W. U., Nóbrega, M., Odegard, M. E., Gomes, B. S., & Dickson, W. G. (2010). Geological and geophysical interpretation of the Rio Grande Rise, south-eastern Brazilian margin: Extensional tectonics and rifting of continental and oceanic crusts. *Petroleum Geoscience*, *16*, 231–245. https://doi.org/10.1144/1354-079309-910

Moulin, M., Aslanian, D., & Unternehr, P. (2010). A new starting point for the South and Equatorial Atlantic Ocean. *Earth-Science Reviews*, *98*, 1–37. https://doi.org/10.1016/j.earscirev.2009.08.001

Peace, A., McCaffrey, K., Imber, J., Phethean, J., Nowell, G., Gerdes, K., & Dempsey, E. (2016). An evaluation of Mesozoic rift-related magmatism on the margins of the Labrador Sea: Implications for rifting and passive margin asymmetry. *Geosphere*, *12*(6), 1–24. https://doi.org/10.1130/GES01341.1

Ranalli, G. (1995). *Rheology of the Earth* (2nd ed.). (pp. 413) New York: Chapmann and Hall.

Rickers, F., Fichtner, A., & Trampert, J. (2013). The Iceland-Jan Mayen plume system and its impact on mantle dynamics in the North Atlantic region: Evidence from full-waveform inversion. *Earth and Planetary Science Letters*, *367*, 39–51. https://doi.org/10.1016/j.epsl.2013.02.022

Rogozhina, I., Petrunin, A. G., Vaughan, A. P. M., Steinberger, B., Johnson, J. V., Kaban, M. K., et al. (2016). Melting at the base of the Greenland ice sheet explained by Iceland hotspot history. *Nature Geoscience*, *9*, 366–369. https://doi.org/10.1038/NGEO2689

Saunders, A. D., Fitton, J. G., Kerr, A. C., Norry, M. J., & Kent, R. W. (1997). The North Atlantic igneous province. *Geophysical Monograph*, *100*, 45–93.

Schellart, W. P. (2004). Quantifying the net slab pull force as a driving mechanism for plate tectonics, *Geophysical Research Letters*, *31*, L07611. https://doi.org/10.1029/2004GL019528

Schlömer, A., Geissler, W. H., Jokat, W., & Jegen, M. (2017). Hunting for the Tristan mantle plume - An upper mantle tomography around the volcanic island of Tristan da Cunha. *Earth and Planetary Science Letters*, *462*, 122–131. https://doi.org/10.1016/j.epsl.2016.12.028

Skogseid, J., Planke, S., Faleide, J. I., Pedersen, T., Eldholm, O., & Neverdal, F. (2000). NE Atlantic continental rifting and volcanic margin formation. *Geological Society of London, Special Publication*, *167*, 295–326.

Torsvik, T. H., Rousse, S., Labails, C., & Smethurst, M. A. (2009). A new scheme for the opening of the South Atlantic Ocean and the dissection of an Aptian salt basin. *Geophysical Journal International*, *177*, 1315–1333. https://doi.org/10.1111/j.1365-246X.2009.04137.x

Torsvik, T. H., Amundsen, H. E., Trønnes, R. G., Doubrovine, P. V., Gaina, C., Kusznir, N. J., Jamtveit, B. (2015). Continental crust beneath southeast Iceland. *Proceedings of the National Academy of Sciences*, *112*(5), E1818–E1827. https://doi.org/10.1073/pnas.1423099112

Turcotte, D. L., & Schubert, G. (2002). *Geodynamics*. Cambridge, UK: Cambridge Univ. Press.

Zhao, D. (2007). Seismic images under 60 hotspots: Search for mantle plumes. *Gondwana Research*, *12*, 335–355. https://doi.org/10.1016/j.gr.2007.03.001